Tropospheric nitrogen dioxide levels vary diurnally in Asian cities

Junsung Park[1,2+], Hyunkee Hong[3+], Hanlim Lee[1*], Si-Wan Kim[4,5*], Jhoon Kim[4], Michel Van Roozendael[6], Caroline Fayt[6], Myong-Hwan Ahn[7], Daniel J. Jacob[8], Seunghwan Seo[4], Kyoung-Min Kim[4], Daewon Kim[1,9], Wonei Choi[1,10], Won-Jin Lee[3], Dong-Won Lee[3], Thomas Wagner[11], Andreas Richter[12], Nickolay A. Krotkov[13], Lok N. Lamsal[13,14,15], Dai Ho Ko[16], Seung Hoon Lee[16], Jung-Hun Woo[17]

[1]Division of Earth Environmental System Science, Major of Spatial Information Engineering, Pukyong National University, Busan, Republic of Korea
[2]Center for Astrophysics | Harvard & Smithsonian, Cambridge, Massachusetts, USA
[3]National Institute of Environmental Research, Incheon, Republic of Korea
[4]Department of Atmospheric Sciences, Yonsei University, Seoul, Republic of Korea
[5]Irreversible Climate Change Research Center, Yonsei University, Seoul, Republic of Korea
[6]Belgian Institute for Space Aeronomy (BIRA-IASB), Brussels, Belgium
[7]Department of Climate and Energy Systems Engineering/Social Economy, Ewha Womans University, Seoul, Republic of Korea
[8]Harvard School of Engineering and Applied Science, Harvard University, Cambridge, Massachusetts, USA
[9]Institute of Environmental Studies, Pusan National University, Busan, Republic of Korea
[10]NASA postdoctoral Program (NPP) at Goddard Space Flight Center, Greenbelt, Maryland, USA
[11]Max-Planck Institute for Chemistry (MPI-C), Mainz, Germany
[12]Institute of Environmental Physics (IUP-UB), University of Bremen, Bremen, Germany
[13]Atmospheric Chemistry and Dynamics Laboratory, NASA Goddard Space Flight Center, Greenbelt, Maryland, USA
[14]University of Maryland Baltimore County (UMBC), Baltimore, Maryland, USA
[15]Now at Bureau of Ocean Energy Management, Stirling, Virginia, USA
[16]Korea Aerospace Research Institute, Daejeon, Republic of Korea
[17]Department of Environmental Planning & Advanced Program for Urban Environmental Studies, Seoul National University

+Co-first author. These authors contributed equally to this work.
*Corresponding author: Hanlim Lee (hllee@pknu.ac.kr) and Si-Wan Kim (siwan.kim@yonsei.ac.kr)

Supplementary Figure 1

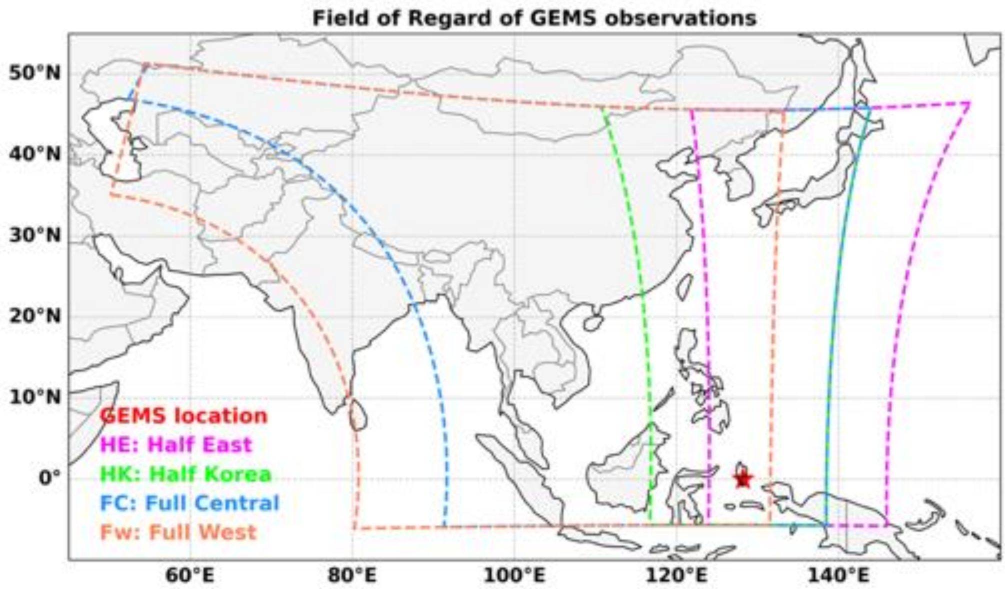

The GEMS observation field of regards depends on the observation mode. Red star represents the location of the GEMS. (pink) Half East; HE, (green) Half Korea; HK, (blue) Full Centra; FC, and (orange) Full West; FW. These modes depended on the GEMS observation schedule (Supplementary Table 1).

Supplementary Figure 2

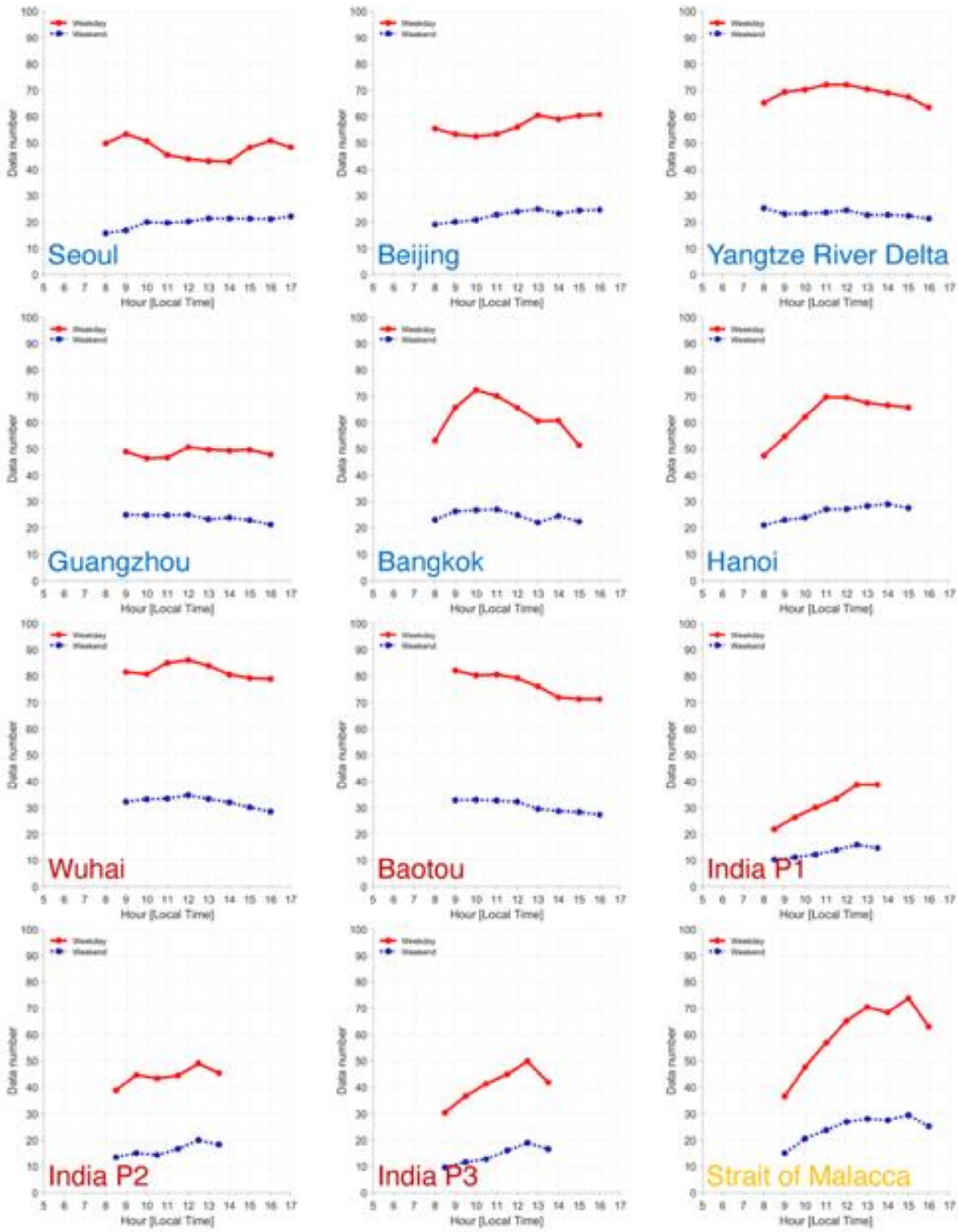

The number of GEMS data used for weekday and weekend averages over the urban regions in Fig. 1. Red and blue lines indicate the number of data for weekdays and weekends, respectively. Blue, red, and yellow labeled regions denote urban, power plant, and ship track sources, respectively.

Supplementary Figure 3

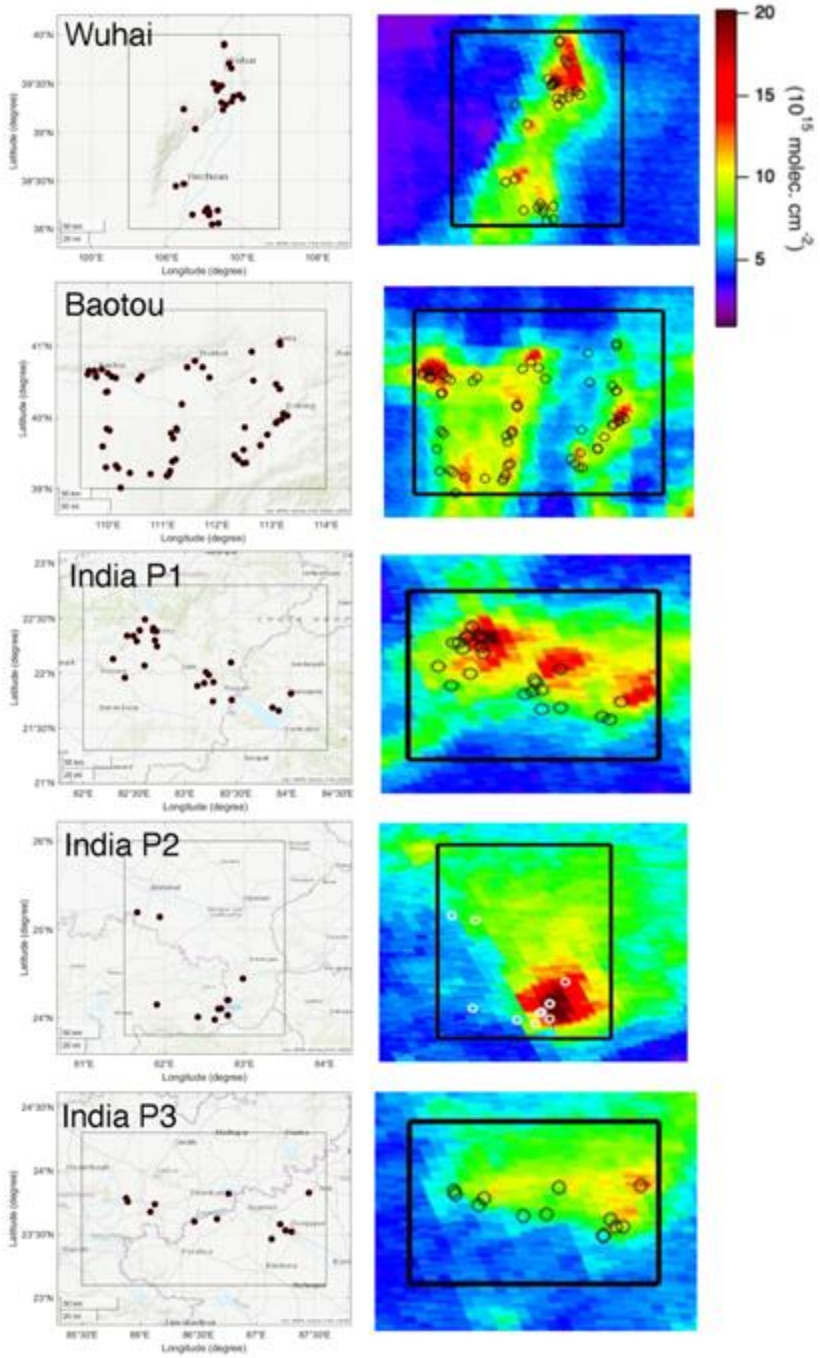

The locations of large power plants (left) and the map of GEMS tropospheric NO_2 columns (right) for the power plant emission dominated regions. The locations of power plants are imbedded in the GEMS NO_2 map.

Supplementary Figure 4

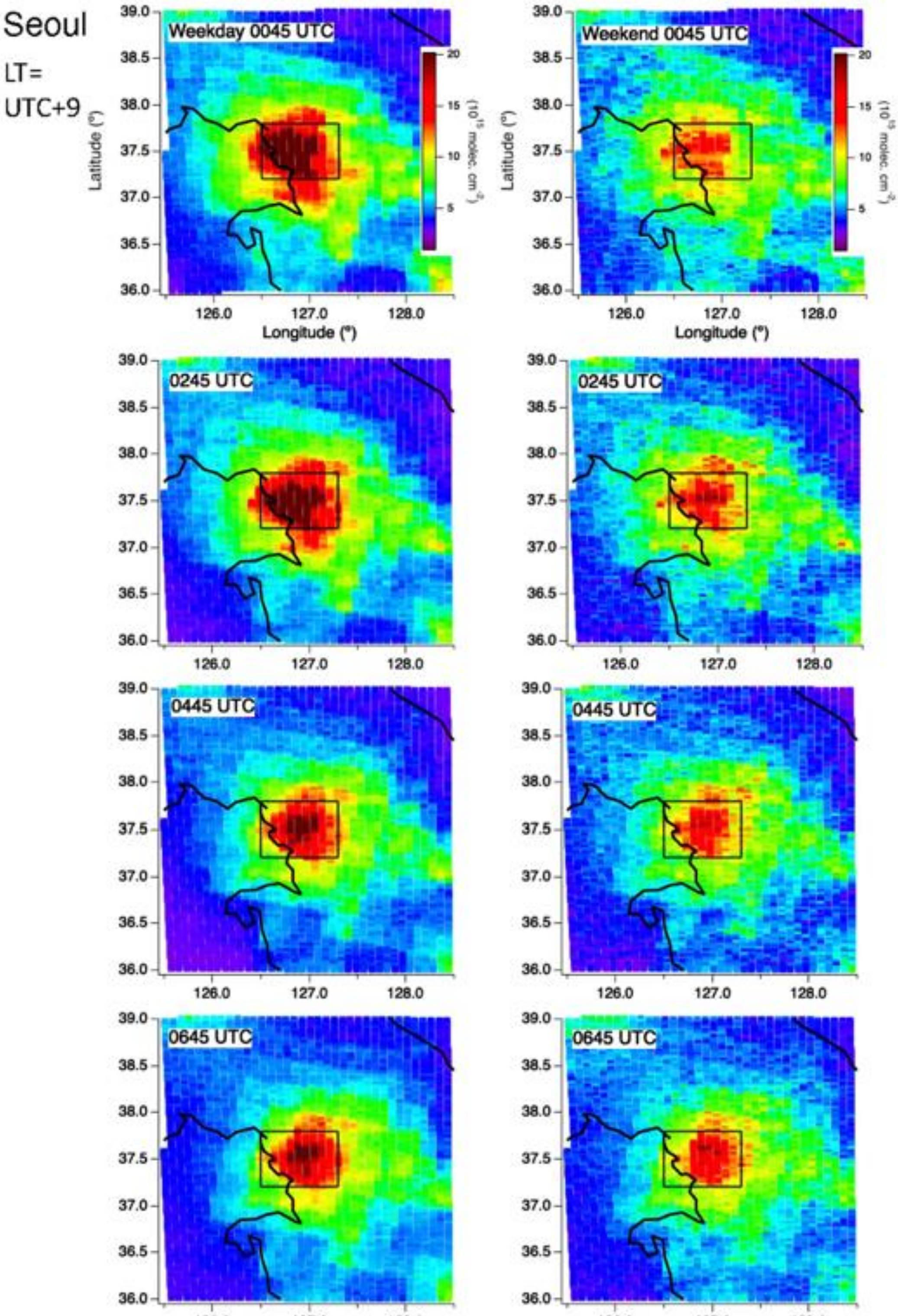

The maps of GEMS tropospheric NO_2 columns over Seoul with time. The left (right) column shows weekday (weekend) value.

Supplementary Figure 5

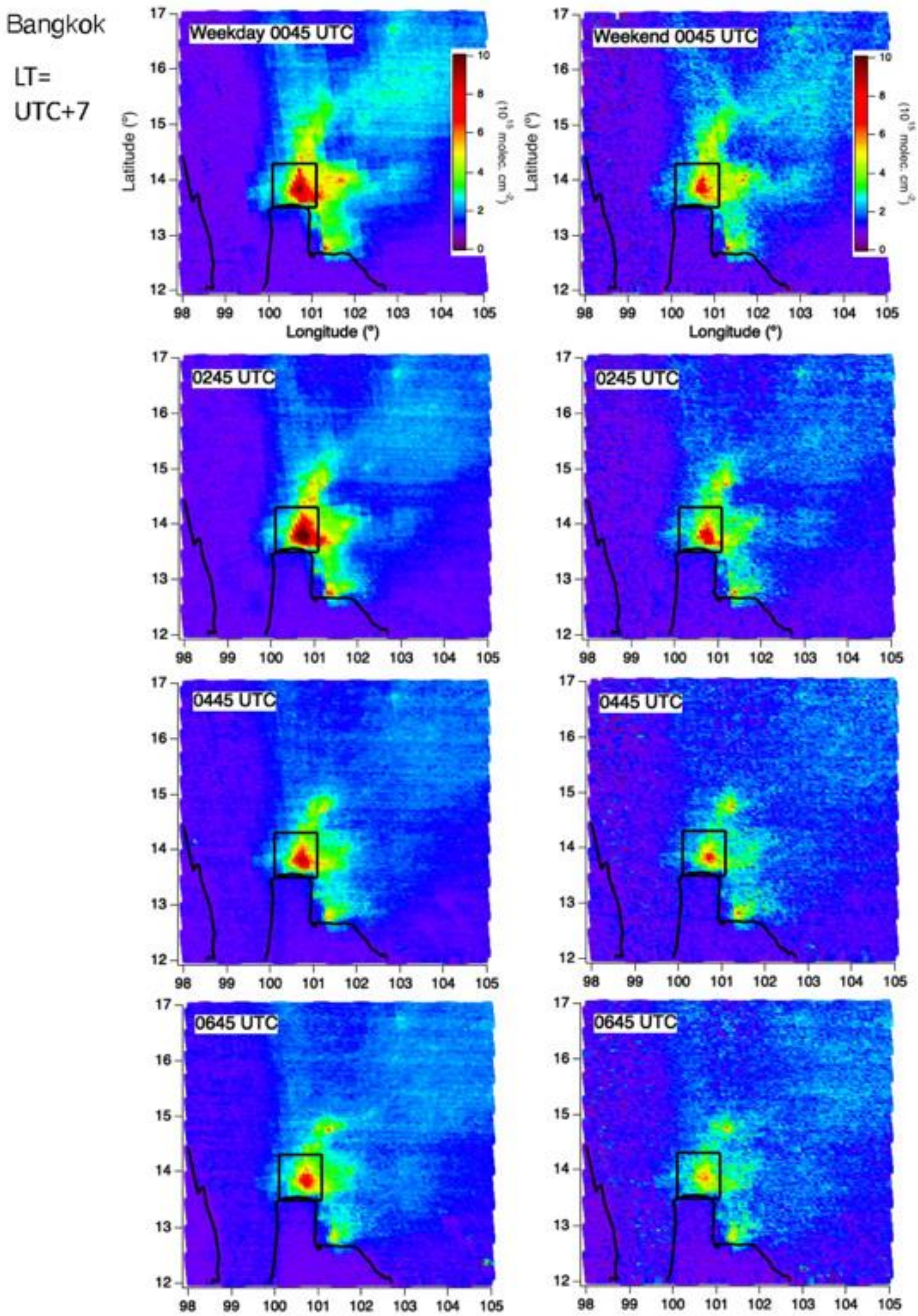

The same as in Supplementary Figure 4 except for Bangkok.

Supplementary Figure 6

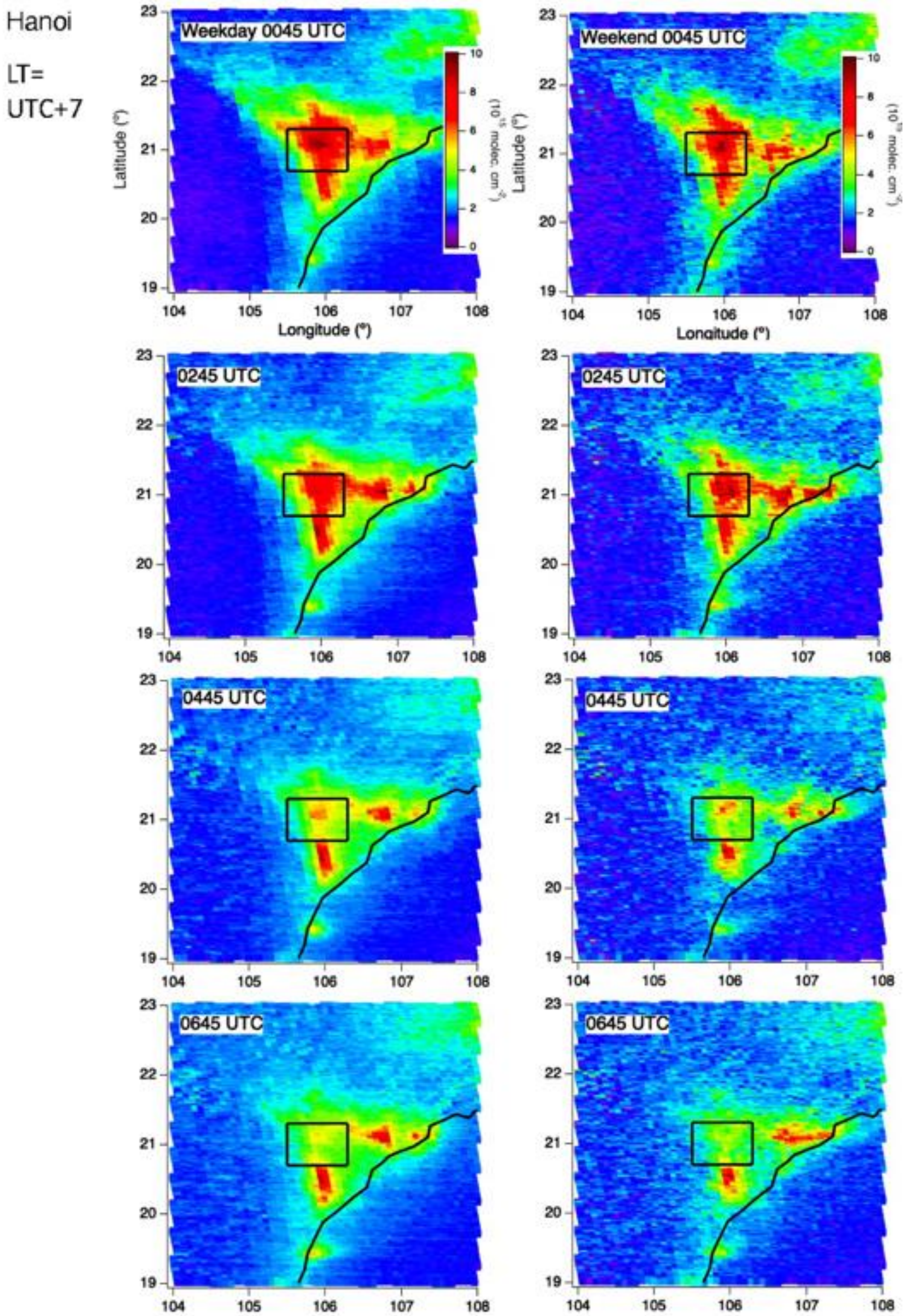

The same as in Supplementary Figure 4 except for Hanoi.

Supplementary Figure 7

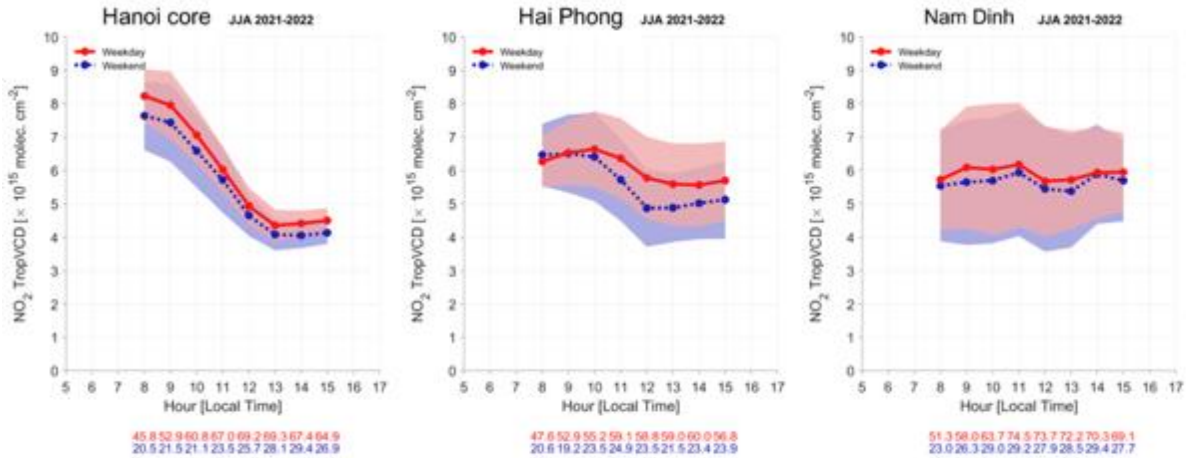

The same as Fig. 1 except for Hanoi core, Hai Phong, and Nam Dinh.

Supplementary Figure 8

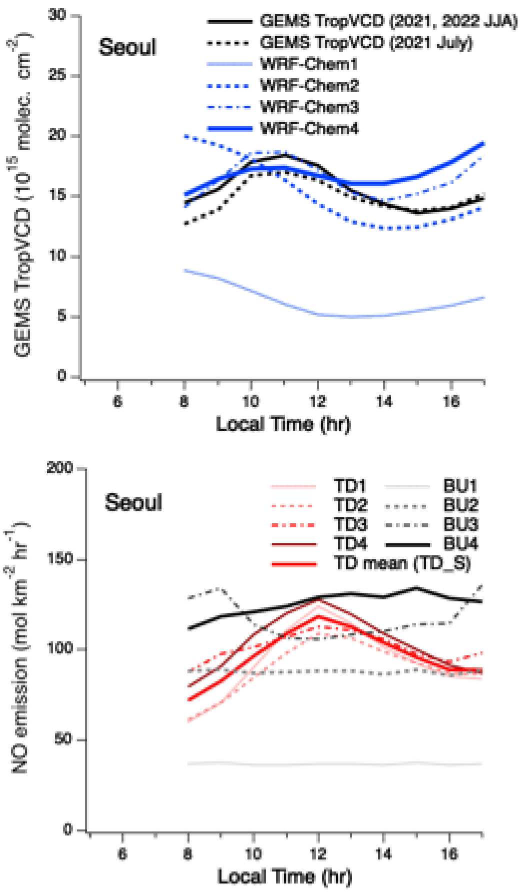

(Top) comparison of GEMS tropospheric NO_2 columns with WRF-Chem model columns, (bottom) comparison of top-down (TD_S) NO emissions with bottom-up (BU) emissions over Seoul. Black solid line in the top plot shows an average of GEMS tropospheric NO_2 columns for the study period (June, July, August of 2021 and 2022) and black dashed line in the top plot represent an average for July 2021. Multiple blue lines in the top plot show the model results using various bottom-up emission options (grey to black lines in the bottom plot). WRF-Chem1, 2, 3, and 4 denote the model columns using BU1, 2, 3, and 4, respectively. All bottom-up emissions are based on AQNEAv2. BU1 is a constant emission that is a nighttime minimum value in BU3. BU2 is a constant emission without applying any diurnal variations as in AQNEAv2. BU3 is the same as BU2 except for utilizing diurnal profile provided by the EDGAR emission. BU4 is the same as BU2 except for applying diurnal profile in previous study[1]. Top-down emissions TD1, 2, 3, and 4 in the bottom plot are derived from the ratios of bottom-up NO emission (BU1, 2, 3, and 4) to the WRF-Chem NO_2 columns. The average of TD1, 2, 3, and 4 (pink to dark red lines) are shown in red bold solid line in the bottom plot.

Supplementary Figure 9

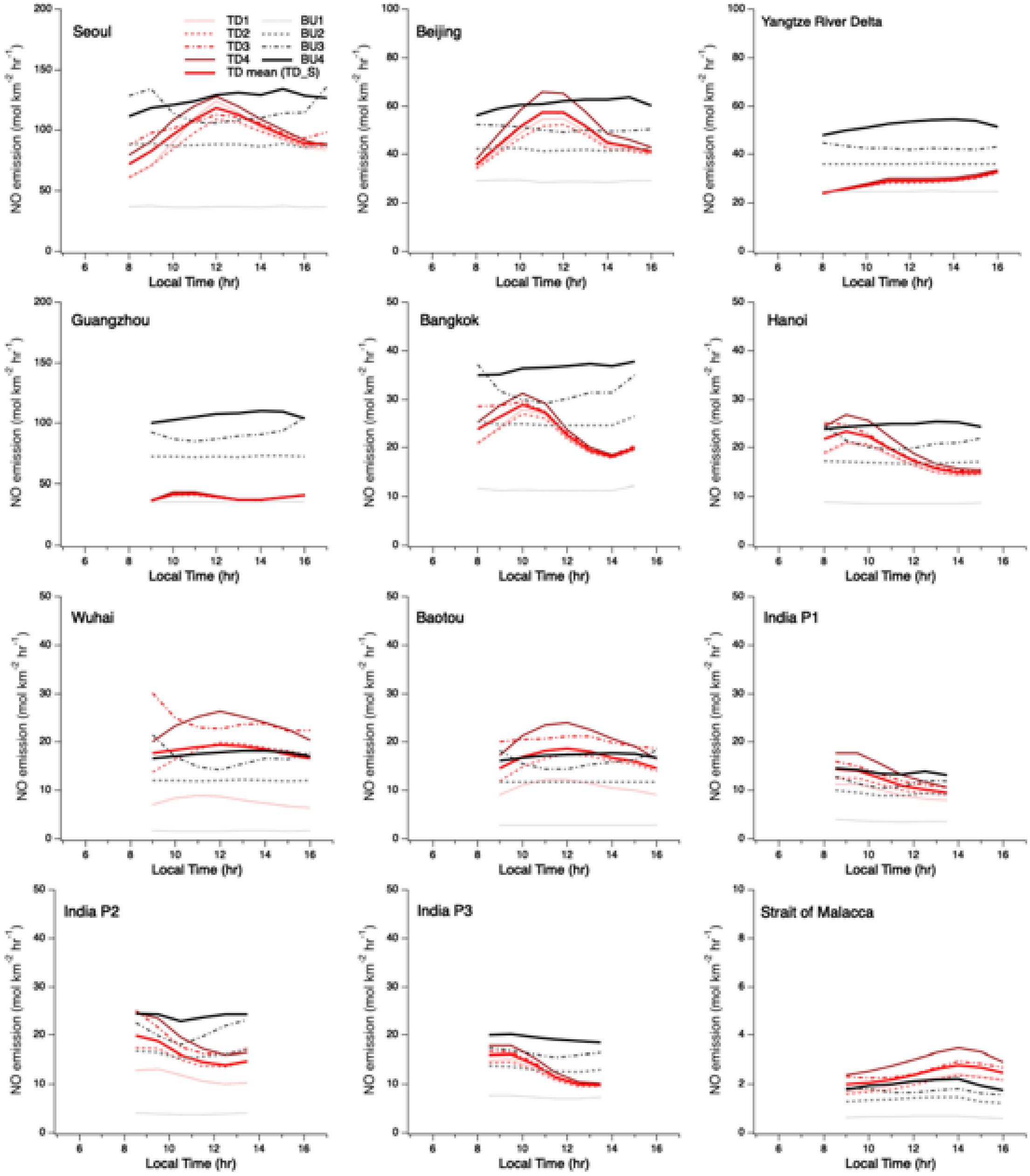

Comparison of diurnally varying top-down emissions with a steady-state assumption (TD_S) (light pink to red lines) with the bottom-up emissions (grey to black lines) over the source regions in this study.

Supplementary Figure 10

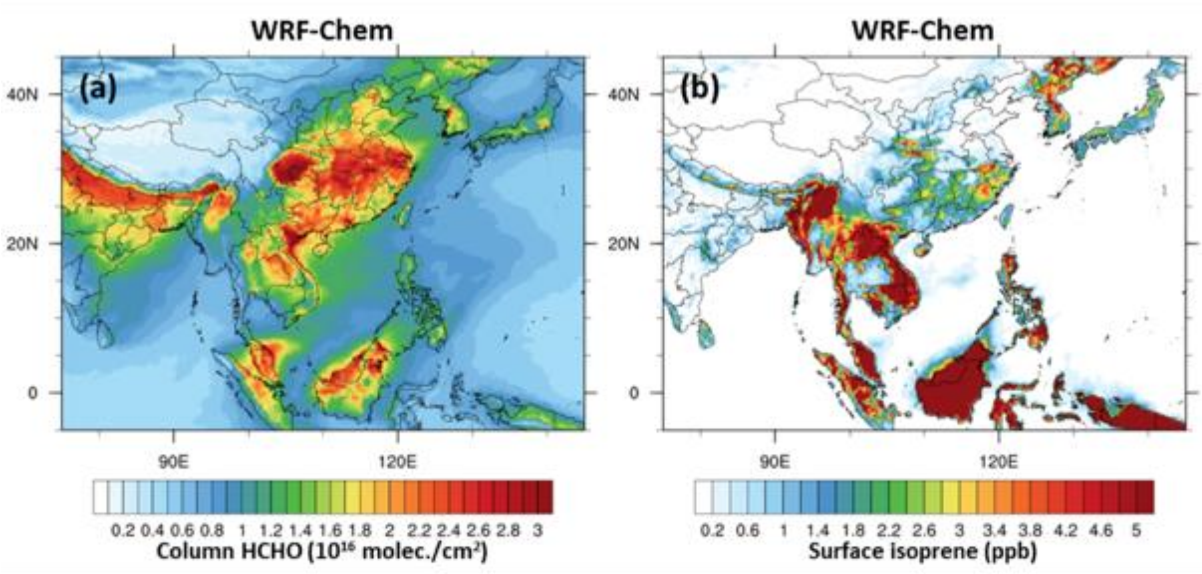

Monthly averaged (a) vertically integrated HCHO and (b) surface isoprene concentrations of WRF-Chem in July 2021 (04:00 to 05:00 UTC).

Supplementary Figure 11

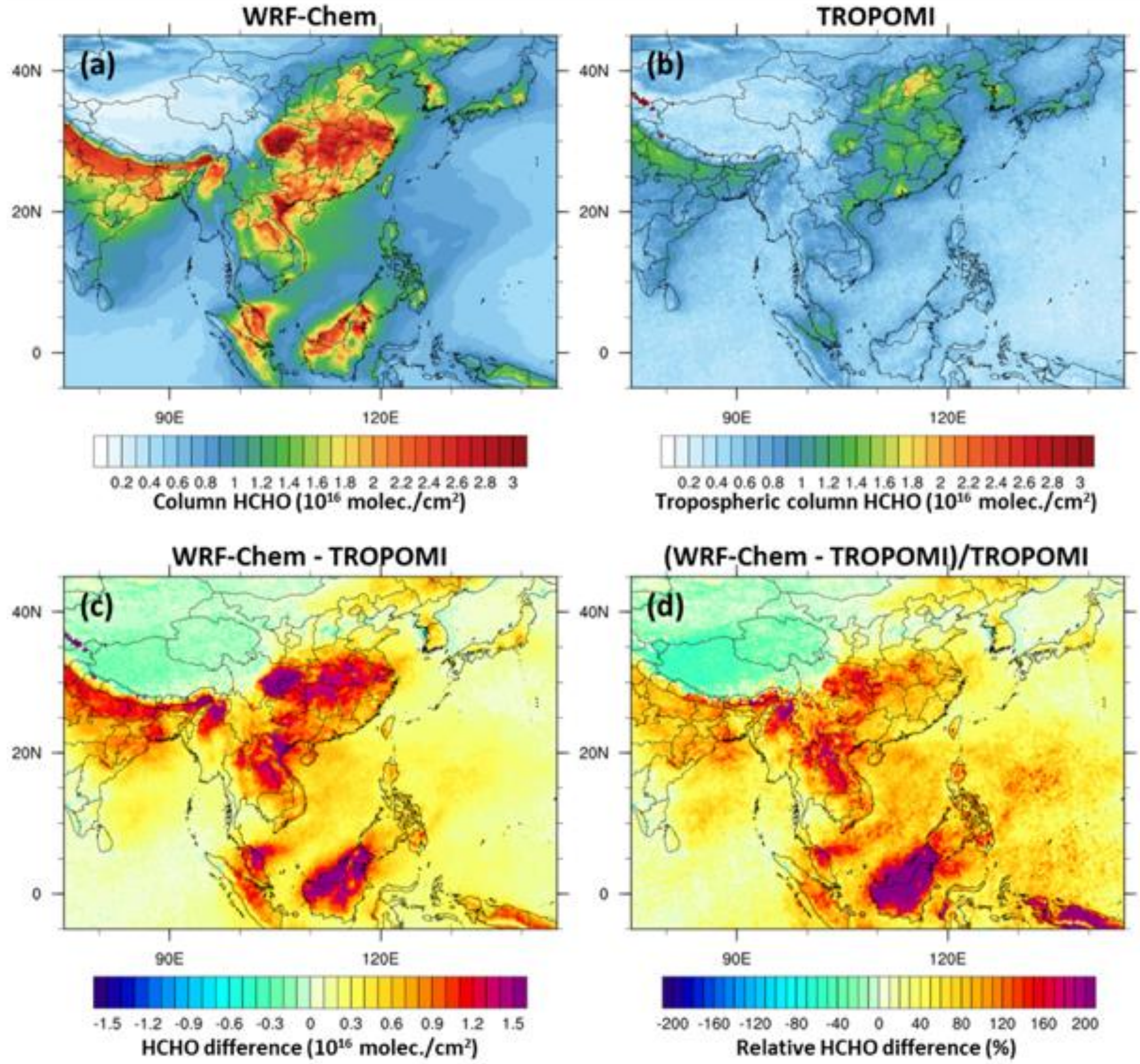

Monthly averaged (a) vertically integrated HCHO concentrations of WRF-Chem (04:00-05:00 UTC) and (b) tropospheric column HCHO concentration obtained from the TROPOspheric Monitoring Instrument (TROPOMI)[2,3] in July 2021 over GEMS domain. The (c) absolute bias and (d) relative difference between WRF-Chem and TROPOMI are presented at the bottom row.

Supplementary Figure 12

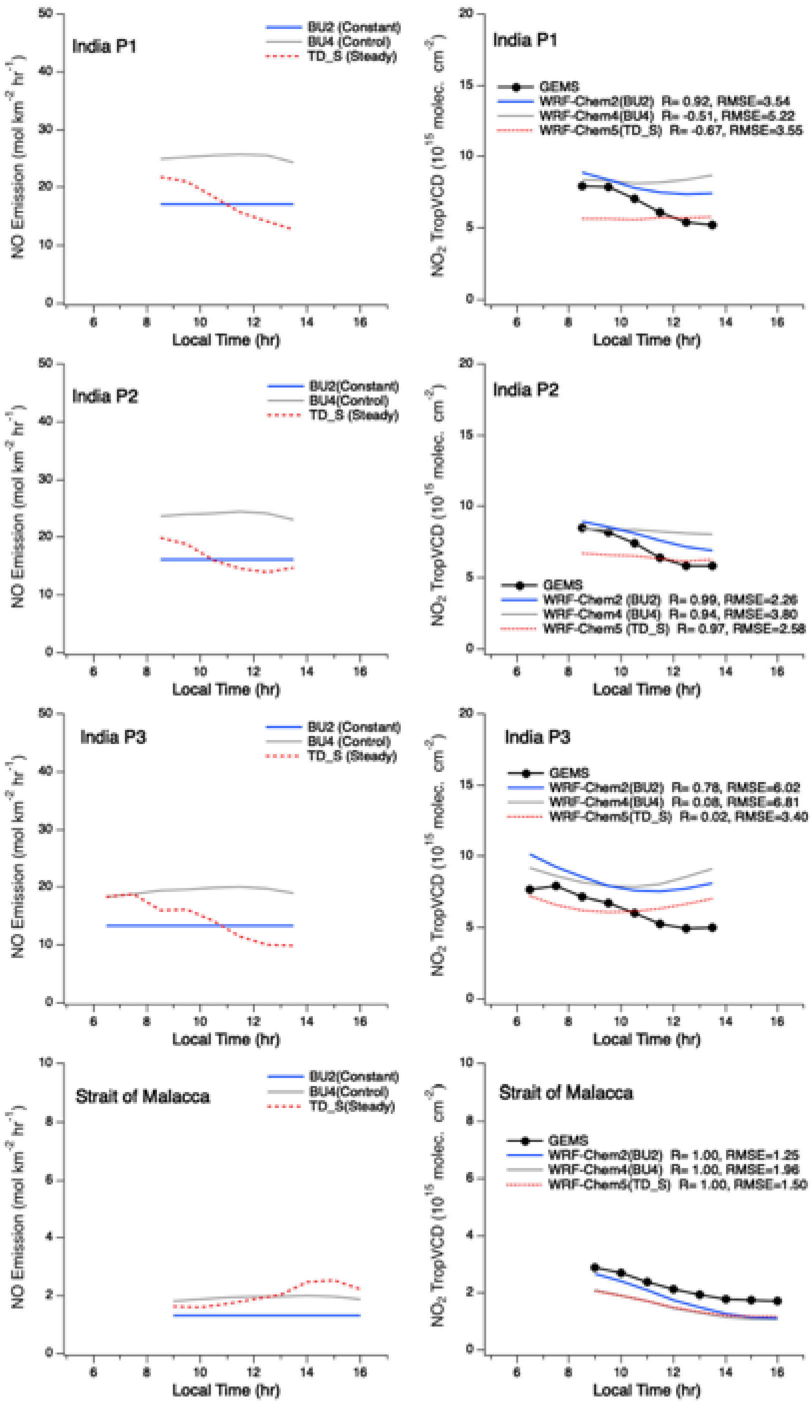

Hourly variations in bottom-up and top-down NO emission (TD_S) (left) and GEMS tropospheric NO_2 columns and model NO_2 columns (right) over India P1, P2, and P3, and the Strait of Malacca during weekdays in the study period. Correlation coefficient and RMSE values are shown on the right panel. The unit of RMSE is 10^{15} molec cm^{-2}.

Supplementary Figure 13

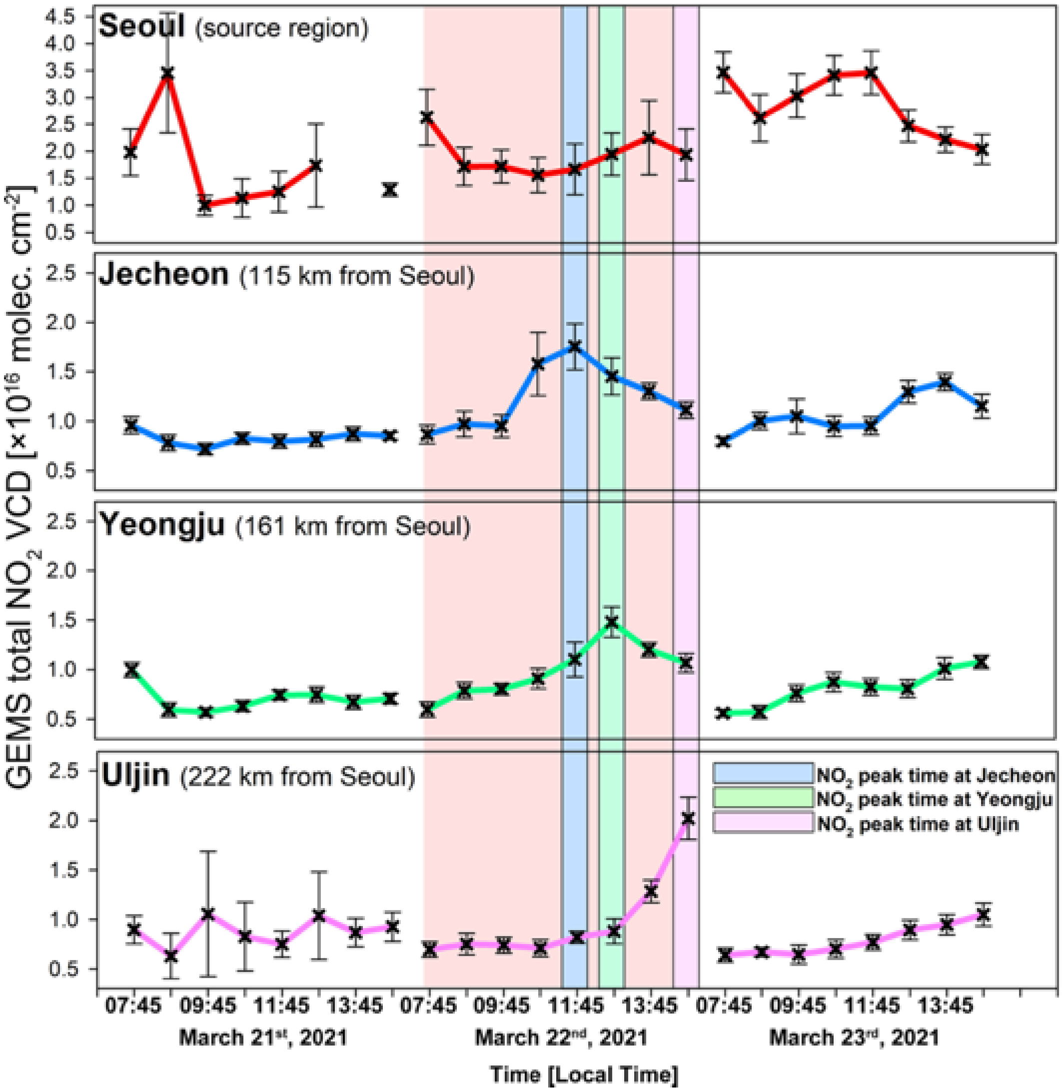

Hourly GEMS NO_2 vertical column density for the receptor cities of Jecheon, Yeongju, and Uljin before March 21, on March 22, and after March 23, 2021. This indicates the transport of NO_2 from the Seoul metropolitan area to various cities. The error bars represent the standard deviation, which was calculated by averaging the pixels located in each region. The red box represents the NO_2 transported event day. The blue, green, and pink boxes indicate NO_2 peak times in Jechen, Yeongju, and Uljin, respectively.

Supplementary Figure 14

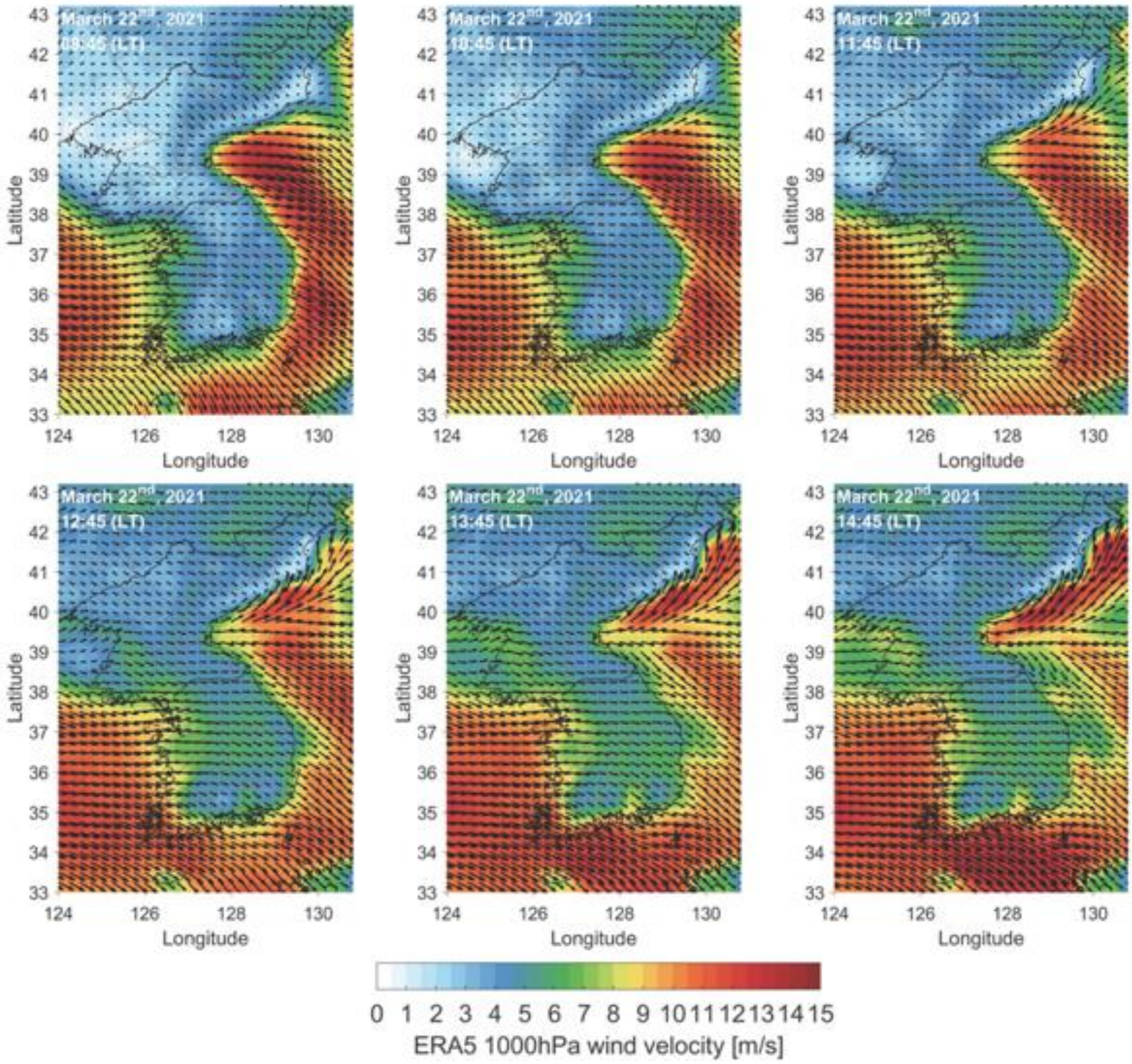

ERA5 wind data for NO_2 transport event over the Korean Peninsula, Korea Strait, and Japan. Hourly ERA5 wind data at pressure 1,000 hPa from 10:00 to 15:00 LT on March 22, 2021, on the Korean Peninsula.

Supplementary Figure 15

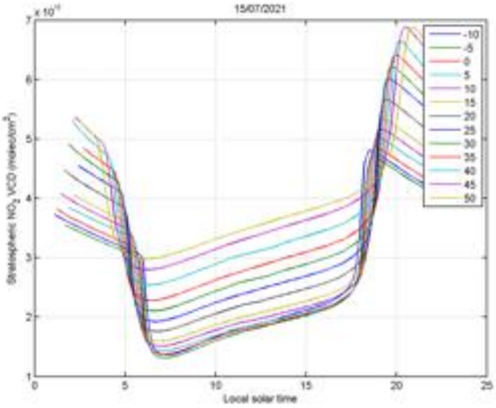

Stratospheric NO_2 vertical column densities as a function of local solar time at various latitude conditions on July 15. Stratospheric NO_2 columns as a function of local time. Solid lines with different colors represent stratospheric NO_2 columns corresponding to the respective latitudes, as represented in the legend.

Supplementary Figure 16

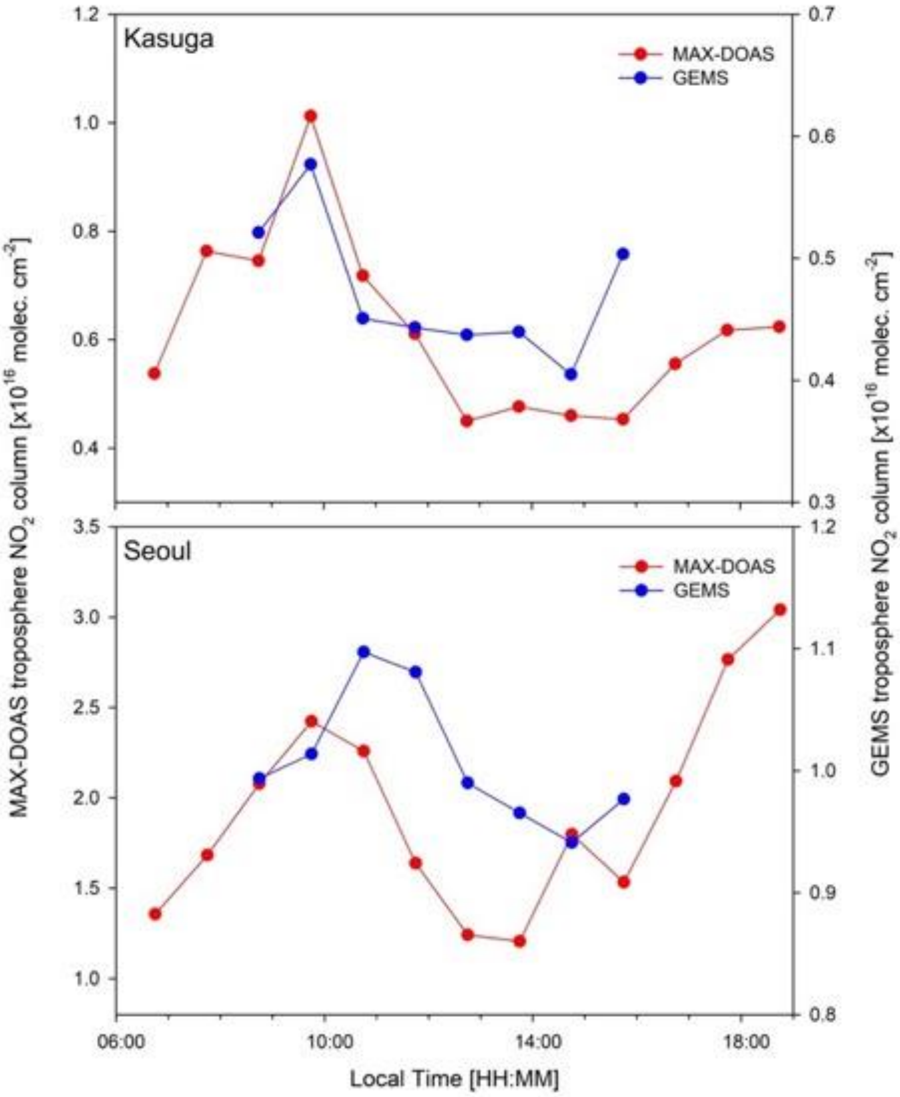

Diurnal variations of monthly averaged tropospheric NO_2 vertical column density retrieved from GEMS and MAX-DOAS observations at (a) Seoul in South Korea and (b) Kasuga in Japan in July 2021. Red dots and lines represent monthly averaged tropospheric NO_2 columns retrieved from MAX-DOAS observations. The blue dots and lines represent tropospheric NO_2 columns from the GEMS observations in July 2021. The left and right y-axes represent the tropospheric NO_2 columns for MAX-DOAS and GEMS, respectively.

Supplementary Figure 17

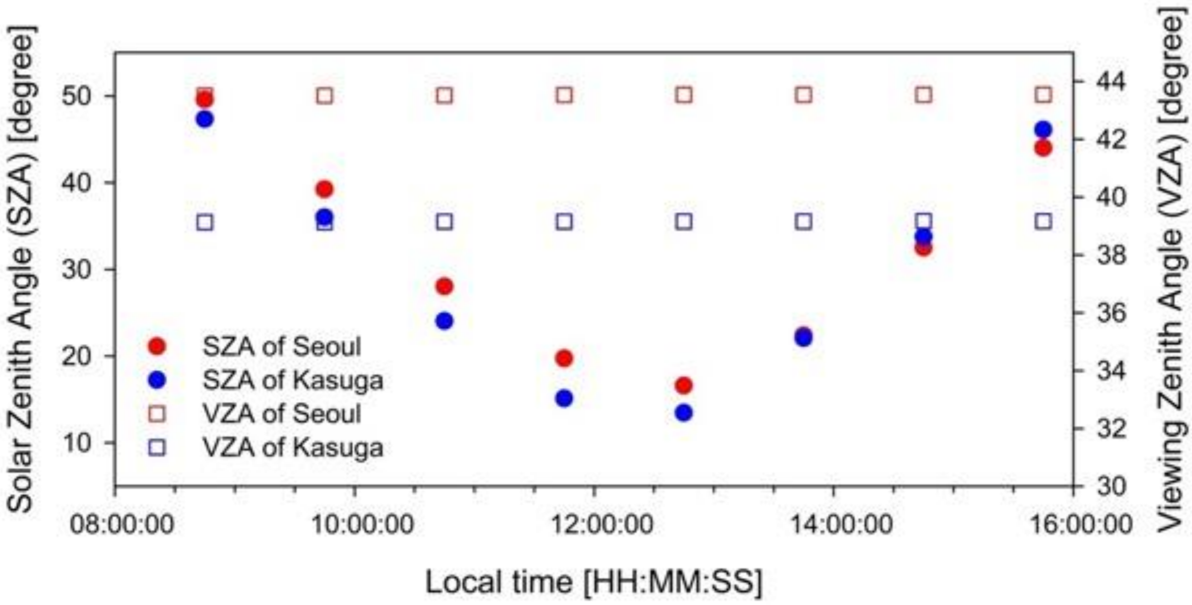

GEMS observation geometry angles at Seoul and Kasuga. The red and blue dots represent the monthly average zenith angles (SZA) in Seoul and Kasuga, respectively, in July 2021. The red and blue rectangles represent the monthly average viewing zenith (VZA) angles in Seoul and Kasuga in July 2021. The left and right y-axes represent the SZA and VZA angles, respectively.

Supplementary Figure 18

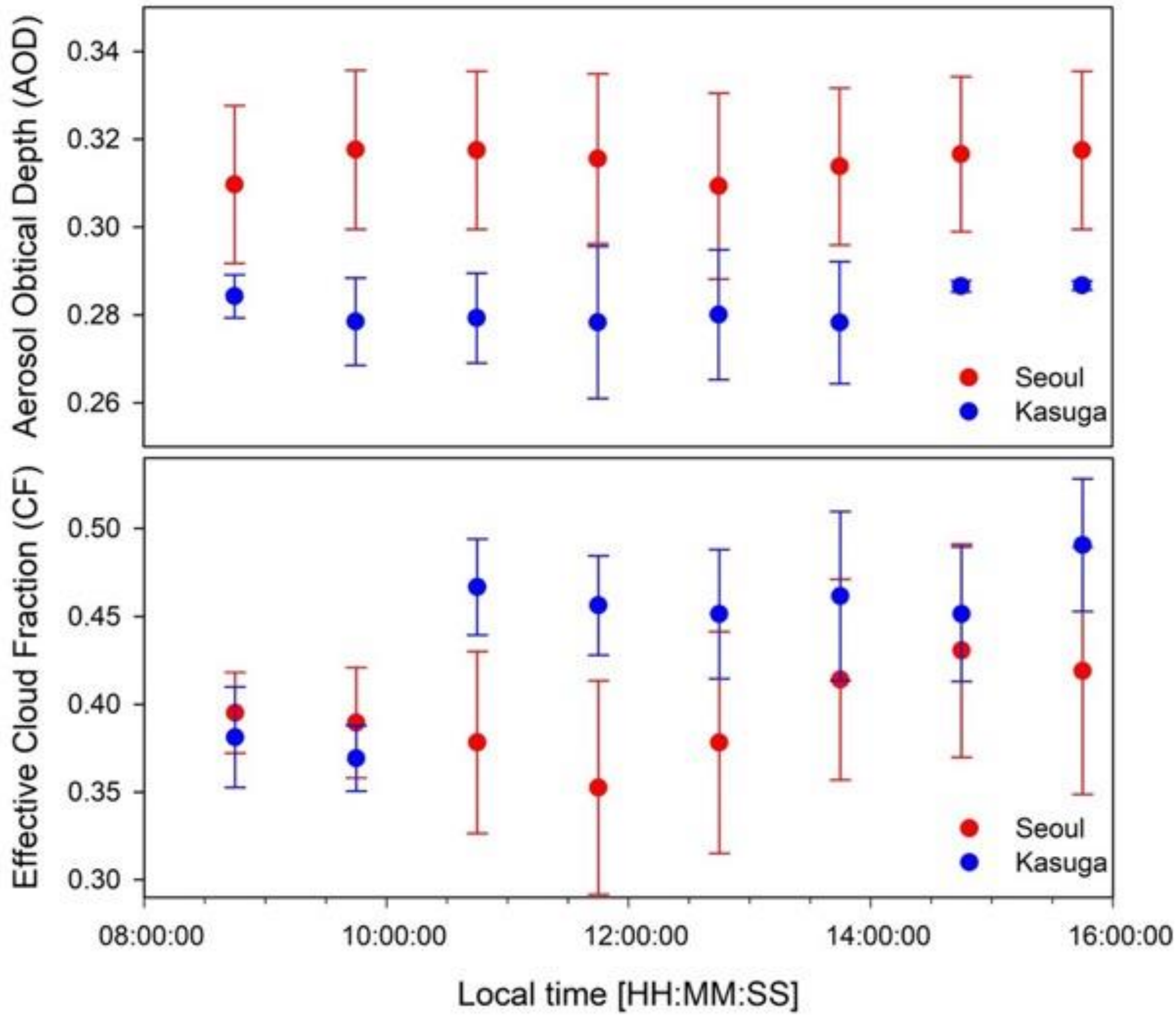

Daytime hourly variation of aerosol optical depth (AOD) and effective cloud fraction (CF) at Seoul and Kasuga, respectively. The red and blue dots in the top panel represent the monthly averaged aerosol optical depth (AOD) obtained from GEMS observations in Seoul and Kasuga in July 2021, respectively. The red and blue dots in the bottom panel represent the monthly averaged effective cloud fraction (CF) obtained from the GEMS observations in Seoul and Kasuga in July 2021, respectively. The error bars represent the standard deviation for each value.

Supplementary figures with the same content as the main figures but using a new color scale:

Figure 2a

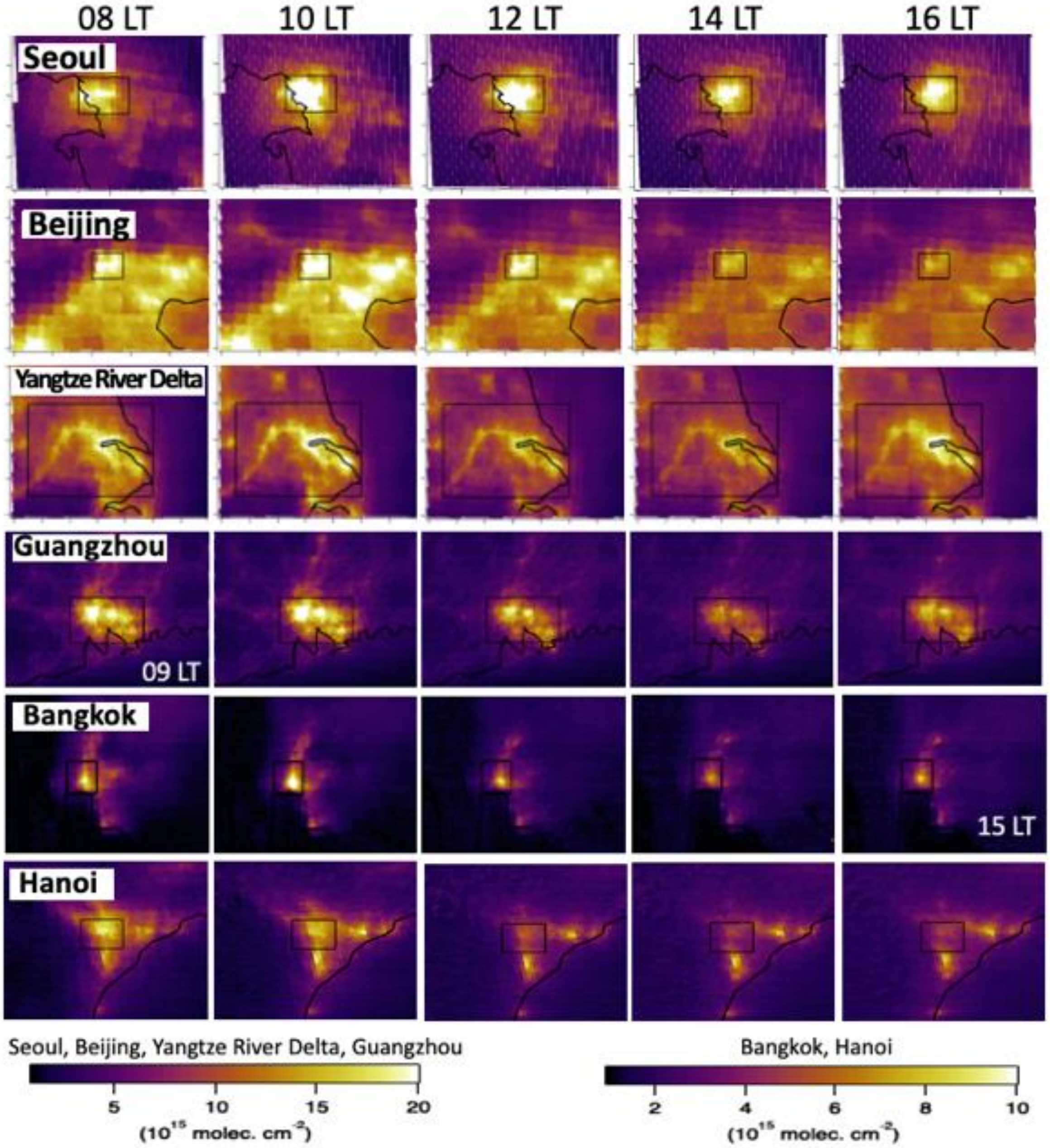

Hourly spatial distribution of average GEMS tropospheric NO_2 columns over major source regions. The observation times are indicated on the top of the plots. Different times are noted in black on the map of Guangzhou (09 LT instead of 08 LT) and Bangkok (15 LT instead of 16 LT) according to the GEMS observation schedule. The latitude and longitude information for each map is provided in Supplementary Data. Approximate local times are shown for each source. The source boxes used for averaging data are exhibited with black rectangles.

Figure 2b

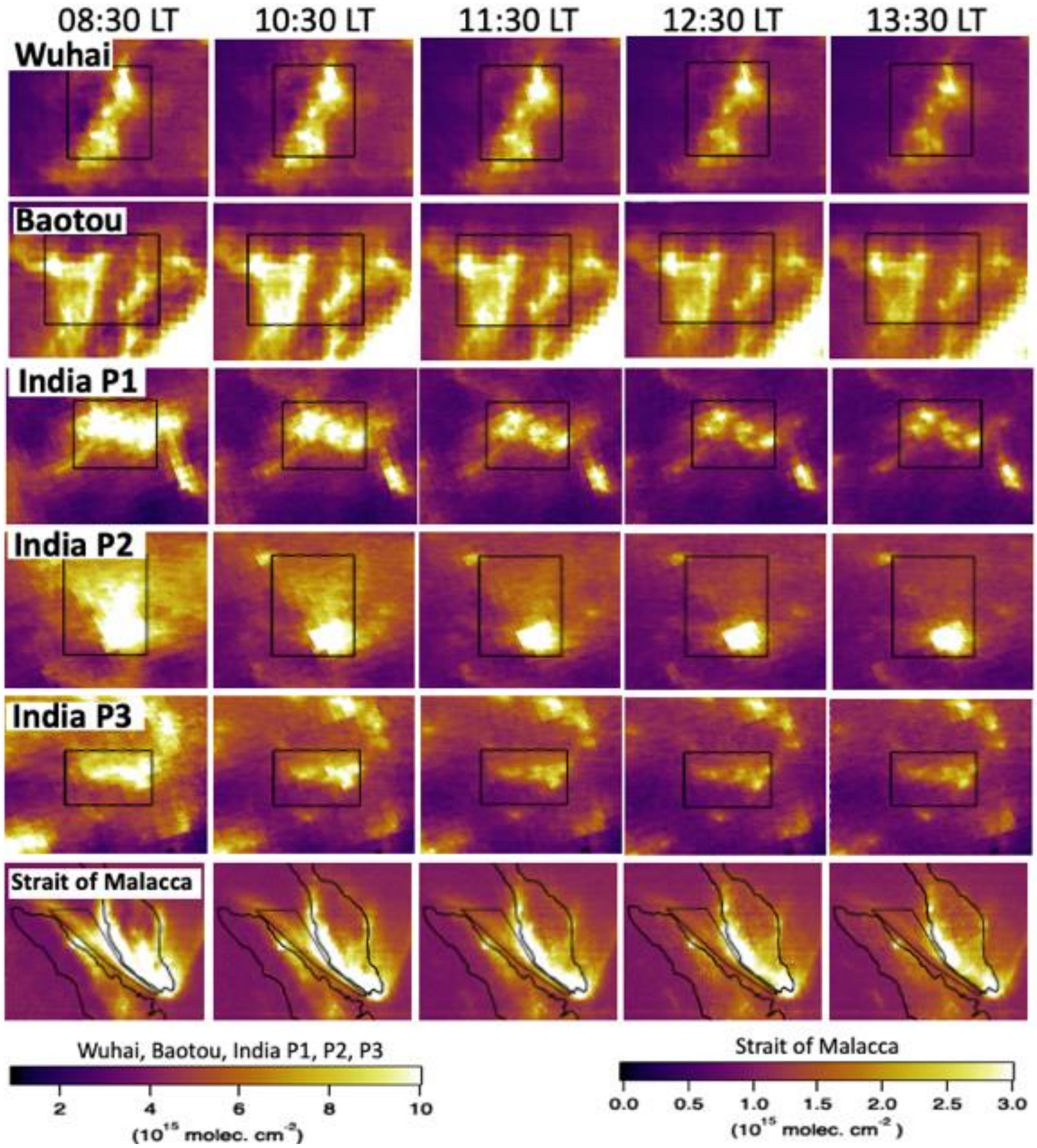

Same as before but for other major source regions.

Supplementary Table 1

GEMS annual observation schedule: HE (Half East), HK (Half Korea), FC (Full Central), and FW (Full West). The observation field of view of these observation modes are shown in the Supplementary Figure 1.

Obs. No.	UTC	JAN	FEB	MAR	APR	MAY	JUN	JUL	AUG	SEP	OCT	NOV	DEC
1	22:45	-	-	-	HE	HE	HE	HE	HE	HE	-	-	-
2	23:45	-	-	HE	HK	HK	HK	HK	HK	HK	HE	-	-
3	00:45	HE	HE	HK	FC	FC	FC	FC	FC	FC	HK	HE	HE
4	01:45	HK	HK	FC	FC	FC	FC	FC	FC	FC	FC	HK	HK
5	02:45	FC	FC	FC	FC	FW	FW	FW	FW	FW	FC	FC	FC
6	03:45	FW	FW	FW	FW	FW	FW	FW	FW	FW	FW	FW	FW
7	04:45	FW	FW	FW	FW	FW	FW	FW	FW	FW	FW	FW	FW
8	05:45	FW	FW	FW	FW	FW	FW	FW	FW	FW	FW	FW	FW
9	06:45	-	FW	FW	FW	FW	FW	FW	FW	FW	FW	-	-
10	07:45	-	-	-	FW	FW	FW	FW	FW	FW	-	-	-
11	08:45	-	-	-	-	-	-	-	-	-	-	-	-
Total Obs. No.		6	7	8	10	10	10	10	10	10	8	6	6

Supplementary Table 2

Information of source location. For the “Strait of Malacca” source, the corner information are listed clockwise from the southwest point.

Source name	Location
Seoul	37.20°N – 37.80°N, 126.50°E - 127.30°E
Beijing	39.60°N – 40.20°N, 116.00°E - 116.80°E
Yangtze River Delta	30.50°N – 33.00°N, 117.50°E - 122.00°E
Guangzhou	22.50°N – 23.50°N, 112.60°E - 114.40°E
Bangkok	13.50°N – 14.30°N, 100.10°E - 101.10°E
Hanoi	20.70°N – 21.30°N, 105.50°E - 106.30°E
Wuhai	38.00°N – 40.00°N, 105.50°E - 107.50°E
Baotou	39.00°N – 41.50°N, 109.50°E - 114.00°E
India P1	21.30°N – 22.80°N, 82.00°E - 84.40°E
India P2	23.80°N – 26.00°N, 81.50°E - 83.50°E
India P3	23.10°N – 24.30°N, 85.50°E - 87.60°E
Strait of Malacca	(103.15°E, 1.324°N), (103.45°E, 1.324°N), (101.40°E, 2.79°N), (99.60°E, 5.50°N), (97.40°E, 5.50°N), (100.70°E, 2.79°N)

Supplementary Table 3

Location of power plants. Data source: Global Energy Observatory, Google, KTH Royal Institute of Technology in Stockholm, Enipedia, World Resources Institute. 2019. Global Power Plant Database v1.2.0. Published on Resource Watch (http://resourcewatch.org/) and Google Earth Engine (https://earthengine.google.com/). Accessed through Resource Watch, (May 31, 2024). www.resourcewatch.org.

Source	Power plant	Latitude (°N)	Longitude (°E)
Wuhai	Alashan Left Qi Wusitai power station	39.4463	106.6676
	CPI Ningxia Zaoquan power station	38.0462	106.6058
	Dongyuan Tech power station	39.4815	106.6882
	Guodian Dawukou power station	39.036	106.3846
	Guodian Shizuishan-2 power station	39.2848	106.788
	Huadian Ningxia Lingwu power station	38.1483	106.3463
	Huadian Wuda power station	39.4794	106.7344
	Huaneng Wuhai Cogen power station	39.707	106.8297
	Huaneng Wuhai Haibowan power station	39.3174	106.865
	Huinong - Yinglite Coal	39.3075	106.7298
	Jingmei Wuhai Jinghai Waste Coal power station	39.6579	106.8622
	Junzheng Wuhai power station	39.4643	106.7014
	Ningdong - Gangue Coal	38.1825	106.5131
	Ningdong Maliantai power station	38.1734	106.5704
	Ningdong Younglight power station	38.192	106.6813
	Ningxia Shizuishan Coal Mine Methane	39.2333	106.75
	Ningxia Wulan Coal Mine Methane	39.2386	106.2297
	North United Power Mengxi power station	39.8926	106.7661
	Ordos Junzheng power station	39.9041	106.7679
	Ordos Power Qipanjing power station	39.3857	106.9657
	Ordos Resources Qipanjing power station	39.3503	107.01
	Shenhua Lingzhou power station	38.1419	106.5665
	Shenhua Wuhai Xilaifeng power station	39.37	106.8927
	Shenhua Yuanyang Lake power station	38.0569	106.691
	Shuidonggou power station	38.2143	106.5439

	Wuda Wuhushan Coal Mine Methane	39.505	106.6267
	Wusitai - Wuda Coal	39.4316	106.6717
	Xixia Ningxia power station	38.4439	106.1258
	Yinchuan power station	38.4677	106.2289
Baotou	Aoweiqianyuan Captive power station	39.2507	111.143
	Baotou Aluminum power station	40.5572	110.1484
	Baotou Donghua power station	40.5781	110.0738
	Baotou East Hope power station	40.5956	109.7828
	Baotou Hexi power station	40.5694	109.79
	Baotou Olefins power station	40.6081	109.6368
	Baotou Works power station	40.6601	109.7585
	Bulian power station	39.3012	109.9682
	CPI Shentou power station	39.5508	112.4887
	Daihai power station	40.5204	112.6674
	Dalate power station	40.367	109.997
	Datang Shentou power station	39.3648	112.5333
	Datang Tuoketuo power station	40.1947	111.3589
	Datang Yungang power station	40.061	113.2192
	Datong - SDIC Coal	39.9474	113.1053
	Datong - Tashan Coal	39.9261	113.0843
	Datong power station	40.0279	113.2933
	Fengzhen - Huaneng Coal	40.4043	113.1446
	Fengzhen - Jinlong Coal	40.4029	113.155
	Fengzhen Xinfeng power station	40.4705	113.0873
	Fugu Qingshuichuan power station	39.2049	111.119
	Great Waste Coal power station	39.4133	112.39
	Guodian Dongsheng power station	39.8228	110.0344
	Hohhot Jinqiao power station	40.7085	111.7399
	Hohhot Jinshan power station	40.7069	111.4576
	Huadian Baotou Tuyou power station	40.5836	110.6228
	Huadian Shuozhou power station	39.3575	112.483
	Huadian Zhuozi power station	40.9221	112.6397
	Huaneng Baotou-1 power station	40.6567	109.6583

Baotou	Huaneng Baotou-2 power station	40.6778	109.8913
	Huaneng Baotou-3 power station	40.6246	110.0028
	Huaneng Hohhot power station	40.7934	111.5977
	Jingneng Energy Huaning Cogen power station	41.0193	113.16
	Jingneng Energy Jining power station	41.0533	113.1533
	Jingtai Zhungeer Suancigou power station	39.7121	111.2012
	Kangbashi power station	39.5978	109.9087
	Mengtai Beijiao power station	39.8465	109.9844
	Ordos Shendong power station	39.3293	110.1518
	Pingshuo Gangue power station	39.4726	112.3225
	Salaqi power station	40.5334	110.5647
	Shangwan Cogen power station	39.2885	110.1905
	Shanxi Yuguang power station	39.6166	112.7998
	Shendong Hequ power station	39.4125	111.244
	Shengle Cogen power station	40.5637	111.8639
	Shenhua Fugu Guojiawan power station	39.2226	110.4066
	Shenhua Fugu power station	39.2092	110.7858
	Shenhua Hequ power station	39.3829	111.1852
	Shenhua Yili power station	40.3614	109.973
	Shenhua Zhunneng power station	39.8279	111.2679
	Shenmu Jieneng power station	39.0121	110.2378
	Tongmei Datang power station	39.9796	113.1859
	Tongmei Tashan power station	39.9792	113.1887
	Tuoketuo 9-10 Coal	40.1892	111.3596
	Wangping power station	39.7637	112.9252
	Xinyuanjieneng Qingshuichuan power station	39.1805	111.0845
	Yonghao Waste Coal power station	39.6103	112.7999
	Youyu power station	39.8663	112.5117
	Zhunda power station	39.7844	111.1595
	Zhungeer power station	39.8535	111.2563
India P1	AKALTARA TPP	21.9603	82.4091
	AVANTHA BHANDAR TPP	21.7438	83.2741
	BANDAKHAR TPP	22.3421	82.4305

India P1	BARADARHA TPP	21.9114	83.1889
	BINJKOTE	22.0103	83.2058
	CHAKABURA TPP	22.3932	82.5532
	I.B.VALLEY	21.6872	83.86
	IND BARATH TPP	21.658	83.92
	KASAIPALLI	22.389	82.5549
	KORBA STPS	22.3881	82.6858
	KORBA-EAST	22.3828	82.7188
	KORBA-WEST	22.4118	82.6888
	LARA	21.757	83.4573
	MARWA TPP	22.0708	82.6022
	NAWAPARA	21.92	83.2788
	PATHADI TPS PH -I	22.2454	82.7246
	RAIGARH TPP	21.9846	83.2331
	RATIJA TPP	22.3404	82.493
	SALORA	22.49	82.6062
	SIPAT STPS	22.13	82.293
	STERLITE TPP	21.8144	84.0404
	SVPL	22.2915	82.5257
	SWASTIK KORBA	22.3005	82.7047
	TAMNAR TPP	22.0987	83.4513
	UCHPINDA TPP	21.8858	83.1215
India P2	ANAPARA "C"	24.2007	82.8
	ANPARA	24.201	82.7891
	MAHAN TPP	24.0077	82.4172
	MEJA STPP	25.1447	81.9415
	NIGRI	24.15	81.9045
	OBRA-A	24.4448	82.9803
	PRYAGRAJ (BARA) TPP	25.196	81.6594
	RIHAND	24.027	82.7915
	SASAN UMPP	23.9784	82.6275
	SINGRAULI STPS	24.1033	82.7068
	VINDH_CHAL STPS	24.0983	82.6719

	BAKRESWAR	23.8285	87.4513
India P3	BOKARO A "EXP"	23.6783	86.0888
	BOKARO B	23.785	85.88
	CHANDRAPURA	23.7376	86.1273
	D.P.L.	23.5211	87.3023
	DURGAPUR	23.531	87.25
	DURGAPUR STEEL TPS	23.58	87.2043
	MAITHON RB TPP	23.8209	86.76
India P3	MEJIA	23.4639	87.1311
	MEJIA TPS EXT	23.4639	87.1311
	RAGHUNATHPUR TPP PH-I	23.622	86.661
	SANTALDIH	23.6013	86.4666
	TENUGHAT	23.7573	85.8936

Supplementary Table 4

The time of maximum and minimum and the ratio of minimum to maximum NO_2 column in GEMS and WRF-Chem results (WRF-Chem2 using constant emission BU2), respectively. The unit of minimum and maximum columns is 10^{15} molec cm^{-2}. P values in the table are calculated from a linear regression test.

Location	GEMS			WRF-Chem with constant emission			P
	Time $_{Max}$	Time $_{Min}$	Ratio of Min to Max (Min, Max)	Time $_{Max}$	Time $_{Min}$	Ratio of Min to Max (Min, Max)	
Seoul	11	15	0.74 (13.6, 18.4)	8	14	0.62 (12.4,20.0)	0.31
Beijing	10	16	0.69 (12.7, 18.5)	8	14	0.54 (15.9,29.5)	0.03
YRD	8	13	0.83 (9.0, 10.8)	8	14	0.71 (13.2,18.7)	0.01
Guangzhou	10	14	0.68 (8.1, 11.9)	9	14	0.80 (18.7,23.5)	< 0.01
Bangkok	9	13	0.75 (3.6, 4.8)	8	12	0.80 (4.7, 5.9)	0.43
Hanoi	8	13	0.60 (3.9, 6.5)	8	13	0.74 (4.6, 6.2)	0.01
Wuhai	11	15	0.79 (4.9, 6.2)	8	15	0.51 (3.5, 6.8)	0.01
Baotou	11	16	0.81 (5.8, 7.2)	8	14	0.65 (5.6, 8.6)	0.20
India P1	8.5	13.5	0.66 (5.2, 7.9)	8.5	12.5	0.83 (7.4, 8.9)	< 0.01
India P2	8.5	13.5	0.68 (5.8, 8.5)	8.5	13.5	0.77 (6.9, 9.0)	< 0.01
India P3	7.5	12.5	0.63 (5.0, 8.0)	6.5	11.5	0.75 (7.6, 10.2)	0.02
Strait of Malacca	9	16	0.59 (1.7, 2.9)	9	16	0.41 (1.1, 2.7)	<0.01

Supplementary Table 5

NO_x chemical lifetime directly calculated (τ_c) and chemical lifetime determined by residuals (τ_r) and OH concentration from WRF-Chem at each location. Averages from 11 LT to 13 LT are shown. τ_c is calculated for chemical loss process forming HNO_3 via a reaction with OH and N_2O_5 heterogenous uptake. τ_r is explained in the Methods section.

Location	τ_c (hr)	τ_r (hr)	OH (pptv)
Seoul	3.0	2.5	0.42
Beijing	2.9	3.3	0.42
YRD	3.8	4.5	0.35
Guangzhou	4.5	4.2	0.29
Bangkok	4.4	3.4	0.29
Hanoi	12.2	4.4	0.11
Wuhai	2.8	3.7	0.62
Baotou	3.9	5.0	0.44
India P1	5.4	6.6	0.27
India P2	4.6	5.9	0.30
India P3	5.3	7.5	0.25
Strait of Malacca	7.2	4.5	0.20

Supplementary Table 6

Validation results (under the condition of GEMS Cloud Fraction (CF) is lower than 0.3). GEMS total NO_2 vertical column densities (VCDs) compared to those of TROPOMI, OMI, and Pandora. Comparison of GEMS tropospheric NO_2 VCDs with TROPOMI, OMI, and MAX-DOAS. Comparisons between the GEMS and TROPOMI and between the GEMS and OMI were conducted for June, July, and August 2021. A comparison between GEMS and Pandora was conducted for the GMAP campaign at Seosan. Additionally, a comparison between GEMS and Panodra was conducted in June, July, and August 2021 at Seoul. A comparison between GEMS and MAX-DOAS was conducted in June, July, and August 2021 at Xianghe.

	GEMS Total NO_2 VCD				**GEMS Trop NO_2 VCD**		
vs	**TROPOMI**	**OMI**	**Pandora**		**TROPOMI**	**OMI**	**MAX-DOAS (Xianghe)**
			Seoul	**Seosan**			
N	580,874	1,201	193	297	225,953	1,148	316
Correlation coefficient (R)	0.78	0.58	0.78	0.66	0.63	0.76	0.51
Slope	1.87	0.58	0.93	0.57	1.27	0.83	0.13
Intercept ($\times 10^{16}$ molec cm^{-2})	-0.36	0.23	0.13	0.51	0.06	0.13	1.42
RMSE ($\times 10^{16}$ molec cm^{-2})	0.18	0.19	0.13	0.32	0.75	0.20	1.31

Supplementary References

1. Seo, S., et al. Reductions in NO_2 concentrations in Seoul, South Korea detected from space and ground-based monitors prior to and during the COVID-19 pandemic. *Environ. Res. Commun.* **3**, 051005 (2021). doi: 10.1088/2515-7620/abed92.

2. De Smedt, I., et al. CCI+P HCHO tropospheric column L3 data from TROPOMI, v1 (Version 1) [Data set], Royal Belgian Institute for Space Aeronomy (2024). https://doi.org/10.18758/2IMQEZ32.

3. Copernicus Sentinel-5P (processed by ESA), 2018, TROPOMI Level 2 Formaldehyde Total Column products. Version 01. European Space Agency (2018). https://doi.org/10.5270/S5P-tjlxfd2.